Energies **2013**, *6*, 3033-3051; doi:10.3390/en6063033

OPEN ACCESS

energies

ISSN 1996-1073

www.mdpi.com/journal/energies

Article

Modeling of a Point Absorber for Energy Conversion in Italian Seas

Silvia Bozzi [1,*], Adrià Moreno Miquel [1,3], Alessandro Antonini [2], Giuseppe Passoni [1] and Renata Archetti [2]

[1] Department of Electronics, Information Science and Bioengineering, Polytechnic Institute of Milan, Piazza Leonardo da Vinci 32, 20133 Milano, Italy; E-Mails: adria.moreno.miquel@gmail.com (A.M.M.); giuseppe.passoni@polimi.it (G.P.)

[2] Department of Civil, Environmental and Materials Engineering, University of Bologna, Viale Risorgimento 2, 40136 Bologna, Italy; E-Mails: alessandro.antonini2@unibo.it (A.A.); renata.archetti@unibo.it (R.A.)

[3] CIRI-EC Fluid dynamics unit, University of Bologna, Via del Lazzaretto 15-5, 40131 Bologna, Italy

* Author to whom correspondence should be addressed; E-Mail: silvia.bozzi@polimi.it; Tel.: +39-02-2399-4146; Fax: +39-02-2399-3360.

Received: 27 March 2013; in revised form: 31 May 2013 / Accepted: 15 June 2013 / Published: 20 June 2013

Abstract: In the present paper, we investigate the feasibility of wave electricity production in Italian seas by the deployment of the Seabased wave energy converter (WEC). A numerical model of the coupled buoy-generator system is presented, which simulates the behavior of the wave energy converter under regular waves of different wave heights and periods. The hydrodynamic forces, including excitation force, radiation impedance and hydrostatic force, are calculated by linear potential wave theory, and an analytical model is used for the linear generator. Two buoys of different radii are considered to explore the effect of buoy dimension on energy conversion and device efficiency. The power output is maximized by adding a submerged object to the floating buoy, in order to bring the system into resonance with the typical wave frequencies of the sites. The simulation results show a very good agreement with the published data on the Seabased WEC. The model is used to estimate energy production at eight Italian offshore locations. The results indicate that the degree of utilization of the device is higher than 20% at the two most energetic Italian sites (Alghero and Mazara del Vallo) and that it can be considerably increased if the floating body is connected to a submerged object, thanks to the resonant behavior of the WEC. In this case, the degree of utilization of the device would be higher than 40% at most of the study sites, with the highest value at Mazara del Vallo. The work enlarges the perspective, to be confirmed by experimental tests and more accurate numerical modeling, on clean electric power production from ocean waves in the Italian seas.

Keywords: wave energy; Italian seas; point absorber; linear generator; simulation

---

1. Introduction

Electricity generation from clean, safe and sustainable energy sources is nowadays a priority for many industrialized countries to meet increased energy demand and to reduce CO_2 emissions. An extremely promising renewable resource, which could provide substantial clean energy supply, is represented by surface ocean waves [1].

Wave electricity production has attracted the interest of governments and industry since the oil crisis of 1973, but wave power technologies are still in the research and development phase [2]. Wave energy faces a number of technical and economic challenges, due to the harsh conditions of the ocean environment, which imply high maintenance and installation costs. Despite the great variety of wave energy converters (WECs) proposed since the pioneering works of Masuda [3], McCormick [4], Budal and Falnes [5], Salter [6] and others, only very few devices have been deployed in real seas. At present, further research is still needed to develop reliable wave power conversion technologies, which could be economically competitive in the global energy market. However, compared to wind and solar energy, wave energy presents considerable technical advantages, because it is more predictable, persistent and spatially concentrated [7]. Moreover, wave energy production has low visual and environmental impact, negligible land use and follows the seasonal variability of energy demand in temperate climates [8]. These favorable aspects of ocean wave energy together with its enormous potential strongly motivate and support the scientific community in finding viable and profitable engineering solutions to capture energy from waves.

Assessments of the global wave energy potential (e.g., [9,10]) show that the most promising locations for wave energy production are off the western coasts of continents in moderate to high latitudes, with a larger proportion in the Southern hemisphere. In Europe, the average annual wave power, expressed as power per unit length of wave crest, increases from 30 kW/m–40 kW/m off the northern Portugal coast [11], up to 75 kW/m off the British Islands [8] and, then, decreases to 30 kW/m off the northern part of the Norwegian coastline [8] and to 5 kW/m off the Swedish west coast [12]. In the Mediterranean basin, the most productive areas are found between the Balearic Islands and the western coast of Sardinia and in the Sicily channel, and they have, respectively, average wave energy fluxes up to 12 kW/m and 9 kW/m [13]. In Italy, an analysis of 18-year wave data measured by the buoys of the Italian Wave Network [14] showed that the most energetic locations are Alghero, on the western coast of Sardinia (9.1 kW/m), and Mazara del Vallo, on the Sicily Strait (4.7 kW/m).

Wave energy conversion technologies can be classified in many different ways: according to the working principle, to the geometry or to the primary location. Recent reviews on the existing wave energy converters can be found in Clément *et al.* [8], Cruz [2] and Falcão [15]. If the horizontal size of the device is much smaller than the typical wavelength, the WEC is called a point absorber; otherwise, it is called a terminator or attenuator, depending on if it is aligned normal or parallel to the prevailing wave direction. Point absorbers (floating or submerged) convert the vertical motion of ocean waves in linear or rotational motion for driving electrical generators by means of a power take off (PTO) system. Point absorbers are very attractive, because they can harness energy from a wavefront much larger than the horizontal width. They operate as the antenna of a radio receiver, which absorbs much more power from the wave than is incident on to its physical cross section [5]. Furthermore, optimal control theory has shown that multiple converters can exploit constructive interference to enhance power absorption [16].

Traditionally, point absorbers have used high speed rotatory machines, such as hydraulic turbines, to extract energy from ocean waves. In recent years, linear generators have been proposed in several marine applications as a well-suited technology [1,17,18]. Direct drive energy converters allow the reduction of the mechanical complexity of the PTO system, obtaining more efficient, reliable and, finally, commercially attractive devices [19]. Many point absorber WECs with linear generators are currently being studied and developed in Europe and North America. Two promising technologies that already reached an advanced development stage are the Archimedes Wave Swing (AWS) device, developed by the company, AWS Ocean Energy [20], and the Seabased's wave energy converter, developed by the Swedish Center for Renewable Electric Energy Conversion of Uppsala University [21]. The AWS consists of a fully submerged air filled chamber, with a lid, which can move vertically with respect to a basement, fixed to the sea bed. As a wave passes over the device, the changes in water pressure induce the movement of the lid, which is linked to a linear generator that converts the motion into electrical energy [22]. The Seabased WEC (Figure 1) consists of a floating buoy connected by a rope to a piston surrounded by permanent magnets [1]. The vertical buoy motion, due to ocean waves, provides piston movement relative to the stator coils, where alternating current is induced. Springs connecting the bottom of the translator to the foundation act as a restoring force and energy storage. Each device has a relatively low power output; hence, the concept is to install several devices in parallel [23].

Figure 1. Sketch of the Seabased wave energy converter.

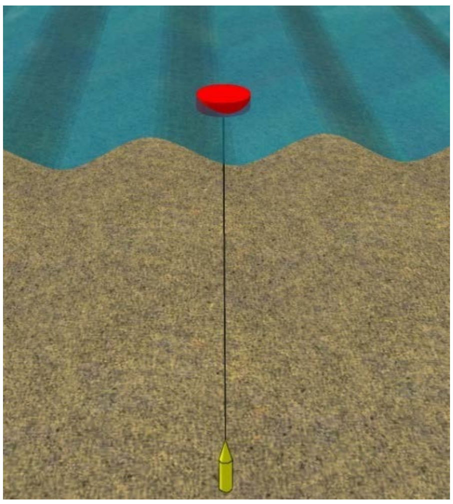

In Italy, wave energy research has been very limited in the last few decades; until the last few years, the only relevant activity has been the development of the resonant wave energy converter (REWEC) by Boccotti [24]. However, rising energy costs and environmental concerns are now pushing the Italian government to increase electricity production by renewable resources. At present, clean energy production covers more than 25% of the state energy demand, a considerably high percentage if compared with the 15% of five years ago [25]. The new interest of the scientific community on wave energy generation has led to some publications on the characterization of the available resource [13,14] and to the first feasibility studies of wave energy exploitation by offshore devices [26–28]. These works showed that the existing technologies that have been designed for more energetic wave climates than the Italian offshore would not be a cost-effective investment in the Italian seas. However, the Italian offshore could be successfully exploited for wave energy production by installing small rated devices specifically designed for areas of moderate wave power, such as the Seabased device.

In the present paper, we investigate the feasibility of wave electricity production in Italian seas by the deployment of the Seabased WEC. This preliminary analysis aims to provide advice for future works, which will involve the design of a point absorber WEC specifically tailored for the Italian wave climate. The behavior of the device is described by the equation of the motion of a single body system restricted to vertical motion. The hydrodynamic forces, including excitation force, radiation impedance and hydrostatic force, are calculated by linear potential wave theory. The generator is simulated based on the analytical model presented by Thornburn *et al.* [29]. Two cylindrical buoys of different radii are considered to explore the effect of buoy dimension on energy conversion and device efficiency. Each buoy is also tuned to be in resonance with the dominant sea states at the study sites, by adding a deeply submerged sphere with neutral buoyancy. Different sea states are simulated to determine the device power output as a function of significant wave height and wave period. Finally, the energy production at eight Italian offshore locations is estimated, and some performance indices are presented. The paper is organized as follows: in the first section, we characterize the wave energy resource of the sea sites considered in the present analysis. In the second section, we describe the mathematical model and in the third section, the buoy configurations, and then, we present the simulation results. Finally, in the last section, some conclusions are drawn.

2. Wave Energy Resource Assessment

Wave energy projects start with the characterization of the wave climate and the wave energy potential. In order to select favorable sites and to design wave energy converters, it is crucial to know the resource availability, its monthly distribution and its composition in terms of sea states.

In this work, we have characterized the wave energy resource of eight locations off the Italian coast, where the wave energy converter is supposed to be deployed. The location of the selected sites is shown in Figure 2. The study sites are wave buoy locations of the Italian wave metric network characterized by wave data records longer than 10 years. The buoys are moored in deep water, at depths ranging from about 60 m in the Adriatic Sea to about 100 m in the Tyrrhenian Sea. Their distance from shore varies between 1.2 km (Crotone) and 15.6 km (La Spezia). Table 1 reports the main features and wave energy statistics of the locations, sorted by decreasing wave power potential (original data from [14]).

Figure 2. Case study locations.

The most energetic sites (1–4 in Table 1) are located in the Tyrrhenian Sea. The average annual wave power at these sites ranges between 3.5 kW/m and 9.1 kW/m, and it is comparable to other sites in the North Sea [2], where wave energy exploitation is at an advanced development stage. The study site with the most energetic wave climate is Alghero, on the western coast of Sardinia. In this location, the annual wave energy is around 90 MWh/m, and the average annual wave power is 9.1 kW/m. The last four sites are located in the Ionian and Adriatic Sea; at all these locations, the annual average wave power is lower than 3 kW/m.

Table 1. Main features and statistics of the study sites. Columns I, II, III and IV represent the percentage of the annual wave energy in the months December–February, March–May, June–August and September–November, respectively.

	Site	Depth (m)	Distance from shore (km)	Wave record length (y)	Missing data (%)	Average annual wave power (kW/m)	CV of average monthly wave power (%)	I	II	III	IV
1	Alghero	95	5.2	18.8	9%	9.1	48%	38%	25%	11%	26%
2	Mazara del Vallo	75	13	18.8	15%	4.7	59%	42%	27%	8%	23%
3	Ponza	100	1.44	17.7	10%	3.7	50%	37%	23%	11%	28%
4	La Spezia	92	15.6	18.8	13%	3.5	36%	33%	23%	14%	30%
5	Crotone	100	1.22	17.5	7%	2.9	56%	47%	23%	4%	26%
6	Monopoli	65	6.02	17.7	9%	2.1	55%	43%	24%	11%	22%
7	Catania	100	5.1	18.8	9%	1.9	63%	43%	28%	6%	24%
8	Ortona	60	10	17.7	12%	1.9	66%	46%	22%	9%	23%

Note: CV, coefficient of variation.

The monthly average wave power strongly varies over the year; the coefficient of variation (CV) of the monthly time series well represents this variation: the most constant sites, in terms of wave power, are located in the Northern Tyrrhenian Sea (La Spezia and Alghero), while the highest variability is found in Catania and Ortona. For all the locations, the most energetic months (December to February, column I of Table 1) provide a large amount of the annual wave energy (varying from 33% of the annual energy in La Spezia up to 47% in Crotone), while the less energetic months (June to August, column III of Table 1) account for a very small percentage of the annual output (only 4% in Crotone). This high seasonal variability, typical of many renewable energy sources, is strongly correlated to wind fluctuations, which are smaller in more temperate zones.

The characterization of the wave climate and the wave energy potential in terms of sea states is shown in Tables 2 and 3. Occurrence of H_S-T_P events, at each location, was obtained from the website of the Italian Wave Network [30]. Table 2 reports the percentage of occurrence and the percentage of annual energy corresponding to different wave height intervals and, Table 3, the percentage of occurrence and the percentage of annual energy corresponding to different intervals of the wave peak period. In the design of the wave energy converter, both the information (percentage of occurrence and percentage of annual energy) should be taken into account; the wave climate data is needed to maximize the degree of utilization (or capacity factor) of the WEC, *i.e.*, the amount of time in a year during which it is operating at its rated power. On the other hand, the bivariate energy distribution is related to the efficiency of the device, which should be maximal for the range of wave height and the period providing the bulk of the energy.

Table 2. Percentage of occurrence (P_O on grey columns) and percentage of annual energy (P_{AE} on white columns) corresponding to different wave height intervals.

H_S (m)	Alghero		Mazara		Ponza		La Spezia		Crotone		Monopoli		Catania		Ortona	
	P_O (%)	P_{AE} (%)	P_O (%)	P_{AE} (%)	P_O (%)	P_{AE} (%)	P_O (%)	P_{AE} (%)	P_O (%)	P_{AE} (%)	P_O (%)	P_{AE} (%)	P_O (%)	P_{AE} (%)	P_O (%)	P_{AE} (%)
<0.5	31.3	0.4	26.8	0.7	38.7	1.4	42.3	1.7	47.2	2.2	43.5	2.8	55.2	4.8	54.1	3.3
0.5–1	27.0	3.3	33.4	8.7	30.9	10.6	34.0	13.1	29.0	11.7	35.3	20.1	30.6	18.7	28.2	16.1
1–1.5	15.0	6.0	19.3	16.0	16.1	17.9	11.9	14.7	12.9	16.7	12.9	22.7	8.4	16.4	10.4	18.2
1.5–2	9.2	8.2	10.7	19.1	7.6	18.5	5.6	14.8	5.8	16.4	4.5	16.6	3.1	13.5	3.7	13.9
2–2.5	6.0	9.8	4.9	15.7	3.6	16.0	2.8	13.3	2.3	11.9	2.0	12.9	1.1	8.7	1.5	10.2
2.5–3	4.0	10.4	2.4	12.7	1.6	11.3	1.6	11.6	0.9	7.9	0.8	8.1	0.5	7.0	0.6	6.4
3–3.5	2.5	9.5	1.3	9.6	0.8	8.2	0.8	8.4	1.0	12.0	0.6	8.6	0.5	10.1	0.7	11.9
3.5–4	1.5	8.1	0.6	6.4	0.4	5.7	0.5	7.5	0.5	8.8	0.3	5.3	0.3	8.6	0.4	9.4
4–5	1.5	11.8	0.5	7.7	0.3	5.9	0.4	8.8	0.4	9.8	0.1	2.4	0.3	9.7	0.3	8.9
5–6	1.4	18.2	0.1	3.0	0.1	3.2	0.1	4.8	0.1	2.4	0.0	0.2	0.0	2.3	0.0	1.3
6–7	0.5	9.9	0.0	0.3	0.0	0.6	0.0	1.0	0.0	0.1	0.0	0.0	0.0	0.2	0.0	0.4
>7	0.2	4.4	0.0	0.1	0.0	0.7	0.0	0.3	0.0	0.0	0.0	0.2	0.0	0.0	0.0	0.0

Table 3. Percentage of occurrence (P_O on grey columns) and percentage of annual energy (P_{AE} on white columns) corresponding to different intervals of wave peak period.

T_p (s)	Alghero		Mazara		Ponza		La Spezia		Crotone		Monopoli		Catania		Ortona	
	P_O (%)	P_{AE} (%)	P_O (%)	P_{AE} (%)	P_O (%)	P_{AE} (%)	P_O (%)	P_{AE} (%)	P_O (%)	P_{AE} (%)	P_O (%)	P_{AE} (%)	P_O (%)	P_{AE} (%)	P_O (%)	P_{AE} (%)
<3	4.3	0.0	3.4	0.1	4.7	0.1	6.7	0.2	6.8	0.2	5.1	0.2	7.1	0.4	9.1	0.3
3–4.5	15.0	0.5	16.6	1.9	26.6	3.1	22.4	3.1	28.5	3.7	26.9	4.6	23.9	3.8	35.6	5.2
4.5–6	25.4	2.8	29.3	9.8	35.6	16.6	24.2	7.8	29.0	13.2	32.7	22.2	22.3	10.9	29.8	21.5
6–7.5	24.7	8.3	27.9	25.1	22.7	30.4	22.1	19.3	19.6	24.1	19.3	33.0	19.2	16.1	15.7	29.4
7.5–9	15.0	15.7	14.3	28.6	7.3	28.4	14.0	29.8	7.9	24.0	7.7	23.7	10.2	20.8	5.0	30.2
9–10.5	9.2	27.9	5.7	24.0	1.7	16.6	7.2	31.0	2.9	24.9	1.8	5.9	4.3	27.9	0.9	10.5
10.5–12	3.5	29.3	1.3	8.6	0.2	2.8	0.9	7.5	0.4	7.4	0.1	0.3	0.9	12.4	0.0	0.1
12–13.5	0.8	14.7	0.1	1.2	0.0	0.8	0.0	0.1	0.0	0.8	0.0	0.0	0.1	2.9	0.0	0.0
13.5–15	0.0	0.5	0.0	0.0	0.0	0.0	0.0	0.0	0.0	0.0	0.0	0.0	0.0	0.0	0.0	0.0
>15	1.9	0.2	1.4	0.7	1.2	1.1	2.6	1.2	4.8	1.7	6.4	10.1	12.0	4.8	3.8	2.7

Wave climate data show that the prevalent sea states are characterized by relatively small waves: in Alghero and Mazara, H_S is below 1 m during approximately 60% of the year, while in the other less energetic locations, the sea states with waves lower than 1 m account for 70%–80% of the time. The peak periods with the highest probability of occurrence are around 6 s for every location, confirming that in the Mediterranean seas, the short waves prevail in the climate.

The comparison between the percentage of occurrence and the contribution to the annual energy shows that most of the annual wave energy is provided by sea states with quite low probability of occurrence. In Table 2, we can see that wave events with H_S lower than 1 m have the largest probabilities of occurrence (between 60% and 80%), but they provide only a small amount of the annual energy (4% in Alghero, between 10% and 15% in Mazara, Ponza, La Spezia and Crotone and around 20% in the last three sites). With regard to wave periods, a large contribution to the annual energy is provided by quite rare events (for example, in Alghero, 29% of the contribution to the annual energy is given by waves with T_P around 11 s, which have a percentage of occurrence of only 3.5%). In the Adriatic Sea, the main contribution to the annual energy is provided by waves with T_P around 7 s, while in the Tyrrhenian Sea, the bulk of the energy is associated with swells with higher periods between 8 s and 11 s, due to the longer fetches.

3. Mathematical Modeling

The wave energy converter is modeled as a single body system with one degree of freedom along the vertical axis (heave mode), as this accounts for most of the movement [31]. The WEC behavior is simulated in the time domain, due to the non-linearity of the PTO system. At this stage, regular waves are assumed. This is the main limitation of the model, because time domain approaches with irregular wave inputs would be more accurate in this context. However, there are indications that the differences between the two approaches are limited, at least for short waves, like those in the Mediterranean Sea [32]. Moreover, our goal was to provide an initial indication of the feasibility of wave electricity production in Italian seas by the deployment of a wave energy converter, designed for mild wave climates. With respect to this scope, we believe that the simplified model of regular waves is adequate and acceptable.

The floating body dynamics are determined by solving the following equation of motion, which combines the hydrodynamic forces $F_H(t)$ and the resistance forces $F_R(t)$ due to the PTO system:

$$m \cdot \ddot{z}(t) = F_H(t) + F_R(t) \tag{1}$$

where m is the total mass of the system and $\ddot{z}(t)$ represents its vertical acceleration.

The hydrodynamic forces on the heaving buoy are calculated by:

$$\begin{aligned} F_H(t) = -m_a\ddot{z}(t) - R_D\dot{z}(t) - \frac{1}{2}\rho A C_D\big(\dot{z}(t) - \dot{\eta}(t)\big)|\dot{z}(t) - \dot{\eta}(t)| - \rho g A z(t) \\ + F_e\frac{H}{2}cos(\omega t + \alpha) \end{aligned} \tag{2}$$

where $z(t)$ is the vertical coordinate at time, t measured with respect to the buoy equilibrium position in calm seas. The five terms on the right side of the equation represent the different forces acting on the buoy: (1) added inertial force, accounting for the fluid volume moving with the buoy, where m_a is the added mass; (2) radiation damping force, due to the waves created by buoy oscillations, where R_D is the radiation damping coefficient; (3) viscous damping force accounting for relative turbulent flow, where ρ is sea water density, A is the waterplane area of the body at rest, C_D is the viscous damping coefficient, set equal to one [33], and $\dot{\eta}(t)$ is the vertical velocity of the free water surface; (4) hydrostatic restoring force, where g is gravity; and (5) vertical component of the excitation force, due to the incident waves on the assumedly fixed body, where F_e is force amplitude, H and ω are, respectively, wave height and frequency and α is the phase angle between the wave and the wave-induced heaving force. The excitation force is usually decomposed into two contributions: the Froude-Krylov force, due to the undisturbed wave field, and the diffraction force accounting for wave deformation, due to the structure. The Froude-Krylov force is considered a reasonable approximation of the excitation force if the body is very small compared with the wavelength [34]. In the present analysis, the full expression of the excitation force is included in the calculations.

The resistance force, $\mathrm{F_R}$, due to the PTO system, is modeled as:

$$F_R(t) = -F_M(t) - F_K(t) \tag{3}$$

where $F_M(t)$ is the electromagnetic force, due to the electric linear generator, and $F_K(t)$ is the elastic force of the spring system attached to the translator, which is calculated by:

$$\mathrm{F_K}(t) = \mathrm{K} \cdot \mathrm{z}(t) \tag{4}$$

where K is the elastic constant of the spring.

The electromagnetic force is obtained through Faraday's law and the Maxwell equations that govern the magnetic induction in the stator-translator structure. The simplified analytical model presented by Thorburn and Leijon [29] is used to calculate the voltage generated in the stator, $e(t)$:

$$e(t) = \frac{2\pi \cdot B_t \cdot w_t \cdot d \cdot p \cdot q \cdot c}{w_p} \cdot \dot{z}(t) \cdot sin\left(\frac{2\pi}{w_p} z(t) - \delta\right) \tag{5}$$

where w_p is the pole width, B_t is the magnetic field in a tooth, w_t is the width of a stator tooth, d is the width of the stator stack, p is the total number of poles, q is the number of slots per pole and phase, c is the number of cables in a slot and δ is the load angle. Through the equivalent electric circuit, the voltage, $U(t)$, and the current, $I(t)$, at the terminals of each phase are, respectively, computed by:

$$U(t) = e(t) - RI(t) - L\frac{dI(t)}{dt} \tag{6}$$

$$I(t) = \frac{R_{load}}{U(t)} \tag{7}$$

where R is circuit resistance, L is circuit inductance and R_{load} is load resistance. Finally, the output power, $P(t)$, and the electromagnetic force, $F_M(t)$, are calculated, respectively, by:

$$P(t) = \sum_{i=1}^{3} U_i(t) \cdot I_i(t) \tag{8}$$

$$F_M(t) = \frac{\overline{\sum_{\iota=1}^{3} U_\iota(t) \cdot I_\iota(t)}}{\dot{z}(t) \cdot \mu} \tag{9}$$

where i is the phase index and μ is the generator efficiency.

4. Simulations

Several cylindrical buoys with different masses and diameters were simulated to investigate the effect of floating body geometry on energy production and device performance. The results indicated that the buoy diameter plays the key role in the process of wave energy absorption, as observed by Waters *et al.* [35]. Hence, we only present here the results of two buoy geometries, characterized by diameters of 3 m (Buoy 1) and 5 m (Buoy 2).

Each buoy was also tuned to be in resonance with the dominant wave frequency of the study sites in order to maximize the power output (Buoy 1sb and Buoy 2sb). A resonant point absorber system has significantly higher power absorption, due to its enhanced amplitude and speed. For small point absorber devices, such as the one studied here, the resonant frequency tends to be much higher than the typical sea state frequency, and so, the resonant state is practically impossible to be achieved. One way to increase the natural period of oscillation of a point absorber is by connecting to the floating buoy a deeply submerged object with neutral buoyancy [36–39]. The additional inertia, due to the submerged body's mass and added mass, allows the decreasing of the natural frequency of the device, which is given by:

$$\omega = \sqrt{\frac{\rho \cdot g \cdot A + K}{\mathrm{m} + \mathrm{m_a}}} \tag{10}$$

where m is the total mass of the WEC and $\mathrm{m_a}$ is the total added mass at the frequency of the incident wave.

Depending on the submerged body mass, the system is tuned to resonate with a different incident wave frequency. Ideally, a different body size should be selected for each study location, to match the local wave climate. In this analysis, following Engström *et al.* [38,39], a spherical body was added as the submerged object, in order to modify the natural frequency of the system. The calculations showed that for the least energetic sites (Crotone, Monopoli, Catania, Ortona), the maximum power output is obtained when the system resonates with waves with peak periods of 5.5 s, while at the most energetic sites (Alghero, Mazara del Vallo, Ponza and La Spezia), the optimum natural period of oscillation ranges between 6 and 7 s. More specifically, it is 7 s at Alghero, 6.5 s at Mazara del Vallo and La Spezia and 6 s at Ponza. Achieving a resonant behavior for such small frequencies implies the use of submerged bodies of very high masses and sizes. As an example, a natural period of oscillation of 7 s would be reached by the use of a submerged sphere of 56 tons for Buoy 1 or 137 tons for Buoy 2. Such bodies are probably unfeasible, because they would damage the electrical and mechanical parts of the wave energy converter. Hence, in this analysis, we tuned the two buoys to be in resonance with waves of peak periods of 5.5 s. The main parameters of the four buoy configurations are reported in Table 4.

For each buoy, the frequency-dependent coefficients of added mass, radiation damping and excitation force were precalculated with the commercial software, ANSYS AQWA [40]. The code is based on the boundary element method and on the linear potential wave theory, which is a suitable approximation for the modeling of point absorbers [41]. The resulting hydrodynamic parameters are shown in Figure 3 as a function of wave angular frequency.

The hydrodynamic parameters of the two body systems were calculated by placing the submerged body at a depth of 25 m. This value was selected after investigating the effect of the distance between the two bodies on the hydrodynamic behavior of the device. Figure 4 shows the hydrodynamic parameters of Buoy 2sb calculated by placing the submerged body at different depths compared to the ones of Buoy 2. It can be noticed that the distance between the floating and submerged body strongly affects the hydrodynamics of the buoy. In particular, if the sphere is placed too close to the free surface, it negatively affects the motion of the surface body, because it drives down the excitation and radiation forces. On the other hand, when the submerged body is well below the motion of the waves, the radiation damping and excitation force coefficients of the single and two-body systems are practically coincident. In this case, the submerged body only contributes to add supplementary inertia to the system without destructively interfering with the floating body.

Regarding the PTO system, a unique parameterization was used for all the simulations. The spring constant was set equal to 6.2 kN/m, *i.e.*, to the value of the first full-scale prototype of Seabased WEC developed at Uppsala University [42]. Table 5 shows the main parameters of the linear generator as reported in the publications of the Swedish Center for Renewable Electric Energy Conversion of Uppsala University (e.g., [42,43]).

Table 4. Main parameters of the buoy configurations.

Parameter	Buoy 1	Buoy 1sb	Buoy 2	Buoy 2sb
Floating body diameter (m)	3	3	5	5
Floating body height (m)	0.8	0.8	1.25	1.25
Floating body draft (m)	0.25	0.25	0.25	0.25
Floating body mass (kg)	1,000	1,000	4,000	4,000
Submerged body diameter (m)	-	3.9	-	5.2
Submerged body mass (kg)	-	31,835	-	74,840
Distance between bodies (m)	-	25	-	25

Table 5. Main parameters of the linear generator.

Parameter	Value	Unit
Nominal power	10	kW
Nominal speed	0.67	kW
Translator length	1.867	m
Stator length	1.264	m
Translator mass	1,000	kg
Width of stator sides	0.4	m
Number of sides	4	-
Pole width	50	mm

Figure 3. Hydrodynamic parameters of the four buoy configurations: (**a**) added mass; (**b**) radiation damping; (**c**) excitation force amplitude.

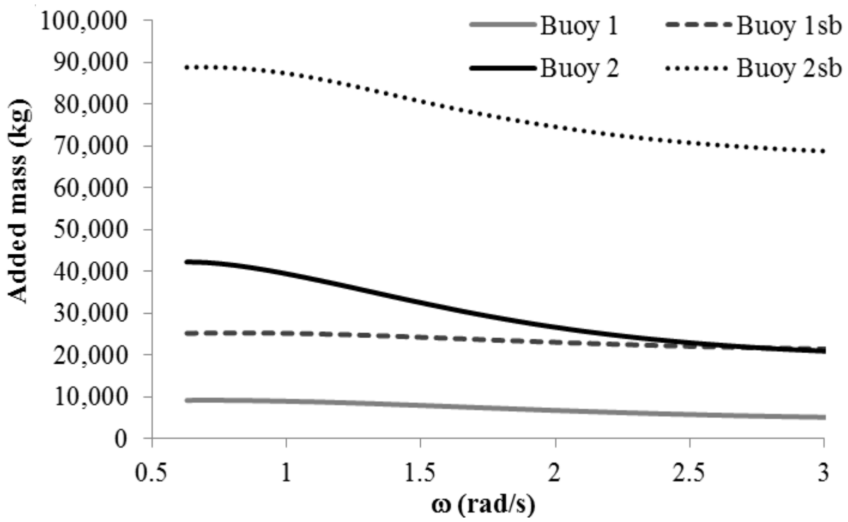

(**a**)

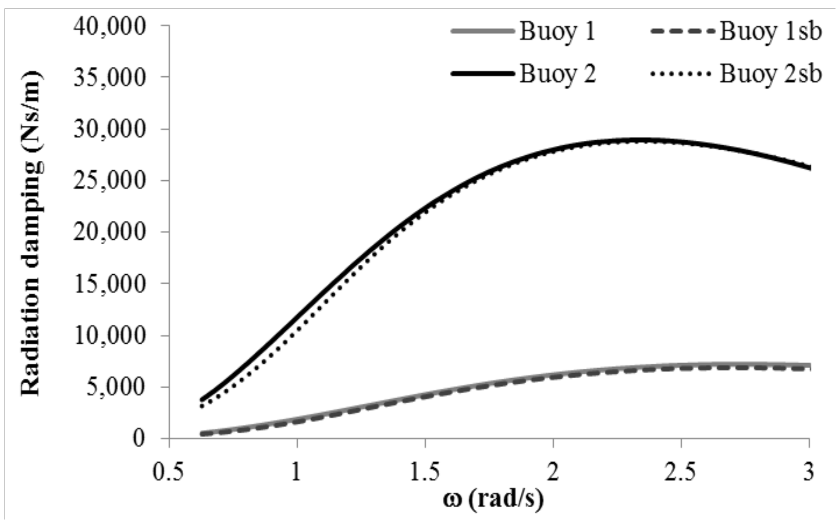

(**b**)

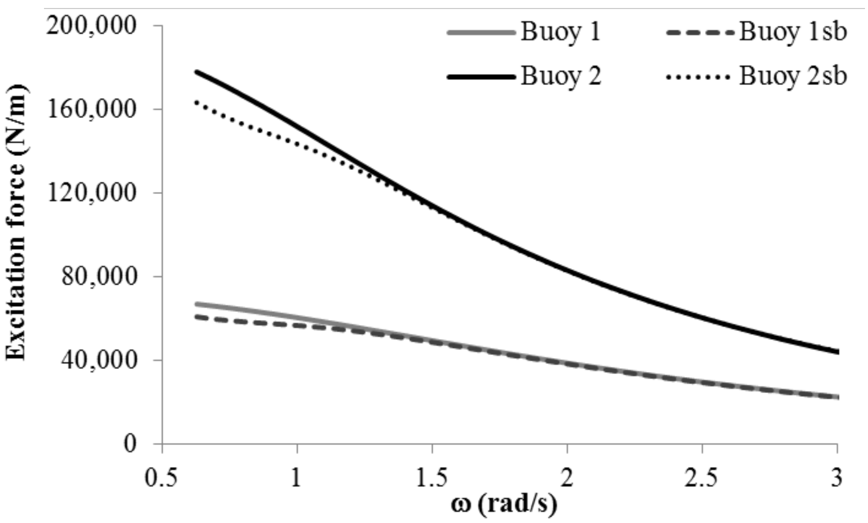

(**c**)

Figure 4. Hydrodynamic parameters of Buoy 2sb calculated with the submerged body at different depths (d = 5 m, d = 10 m, d = 15 m, d = 25 m) compared to the ones of Buoy 2 (No sb): (**a**) added mass; (**b**) radiation damping; (**c**) excitation force amplitude.

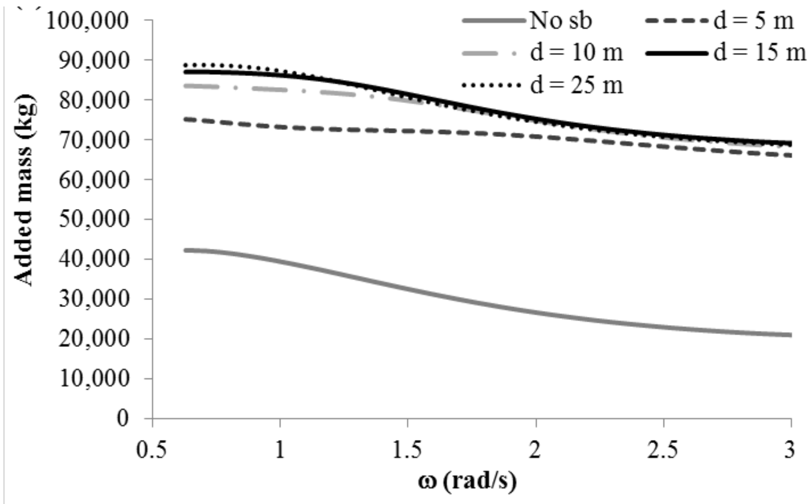

(**a**)

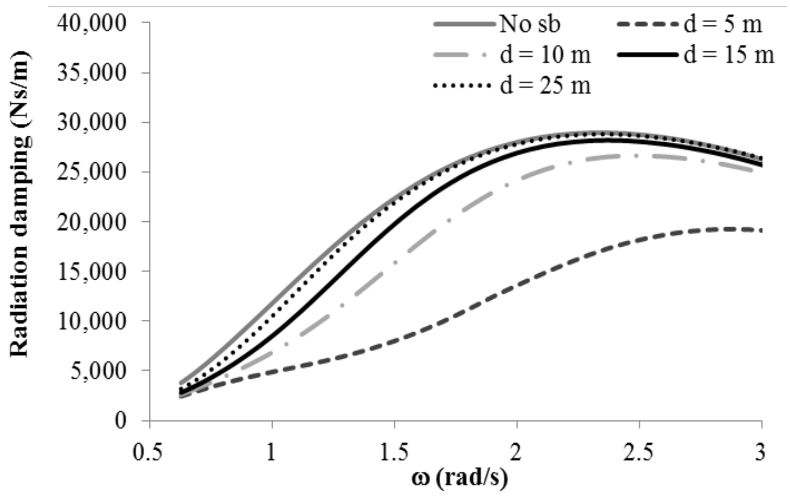

(**b**)

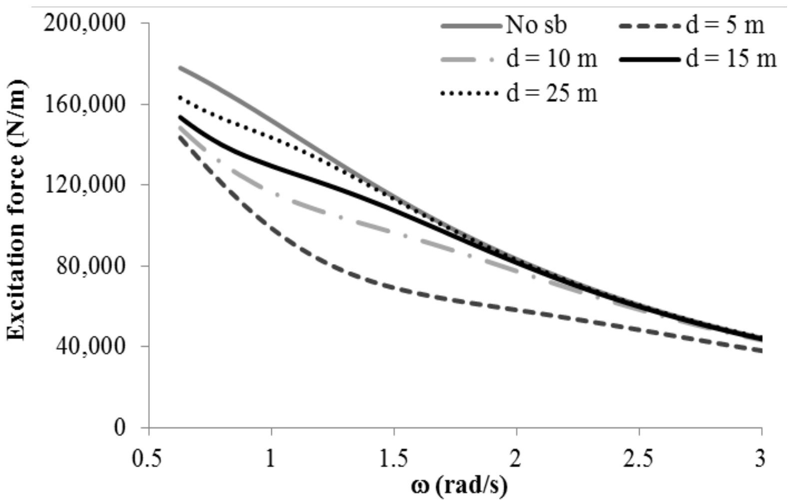

(**c**)

5. Results

The behavior of the wave energy converter was simulated in regular waves of different heights and periods. More specifically, 874 sea states were simulated, considering 38 different significant wave heights (from 0.5 m to 9.5 m) and 23 different energy periods (from 1.5 s to 18 s). The time domain simulations were run until the motion response of the system reached the steady state. The power output of the device was calculated for each sea state to obtain the so-called power matrix, which is a bivariate matrix indicating the average power generated by the WEC as a function of significant wave height and wave period. The comparison of the obtained power matrix with the results presented by Babarit *et al.* [44] for the same device shows a very good agreement.

To evaluate device performance, the capture width ratio of the WEC was calculated for each simulated sea state. The capture width (or absorption width) is a commonly used performance index of wave conversion technologies [45]. It represents the width of the wave front from which energy is extracted, and it is calculated as the ratio of power output to incident wave power per unit of wave front width. The capture width ratio, CWR (or relative capture width), is the capture width divided by device width, and it was computed by the following expression:

$$\mathrm{CWR} = \frac{\mathrm{P_{abs}}}{\mathrm{J} \cdot \mathrm{D}} \tag{11}$$

where $\mathrm{P_{abs}}$ is mean absorbed power, D is device width, and J is wave power per unit of wavefront length, which is given by:

$$\mathrm{J} = \frac{1}{64\pi}\rho g^2 \mathrm{H_S^2 T_e} \tag{12}$$

where T_e is the energy period. The energy period is defined as the period of a single sinusoidal wave that would have the energy of the sea state, and it is calculated as the ratio between the spectral moment of order the -1 and of the order zero. Figure 5 shows the capture width ratio of the buoy configurations as a function of significant wave height (Figure 5a) and energy period (Figure 5b).

The capture width data of the single body configurations (Buoy 1 and Buoy 2) agree very well with the results published by the Uppsala University Research Group, confirming the model's ability to reproduce system behavior and performance. In particular, the device performance decreases with increasing wave height, for H_S higher than 0.5 m, as reported by Tyrberg *et al.* [43], and it decreases with energy period for T_e longer than 4.5 s, as noticed by Waters *et al.* [35]. The region of maximum efficiency corresponds to the sea states with H_S between 0.5 and 1 m and T_e between 4 and 5 s, in agreement with Waters *et al.* [35]. Moreover, it can be noticed that the efficiency of the wave energy converter decreases as the buoy size increases. Also, it can be observed that the differences in the capture width ratio are higher in the area of maximum device efficiency. This does not imply that the smaller buoy extracts more energy (in fact, the opposite is true, as shown in Figure 6a), but it means that it can capture a higher percentage of the wave power incident upon its width.

The two body configurations have a significantly higher capture width ratio for all the sea states. As expected, the maximum power absorption is achieved for waves with energy periods of 5.5 s, which bring the system into resonance. As the wave period increases, the capture width ratio decreases, much more rapidly than in the single body system. This was already observed by Engström [39].

Electricity production of the four devices was estimated by multiplying the expected power output of each sea state (defined by H_S, T_p pairs) by its occurrence (in hours), for each study site. Then, the energy of each sea state was summarized to obtain the mean annual energy extracted by the devices at each location (Figure 6a). From these data, the average degree of utilization and capture width ratio of the WECs were estimated (Figure 6b,c). The degree of utilization is the ratio of the average power output by the rated output (10 kW), and it is one of the most important indices of the economic convenience of a renewable energy technology [46,47].

Figure 5. Capture width ratio of the buoy configurations as a function of (**a**) significant wave height and (**b**) energy period.

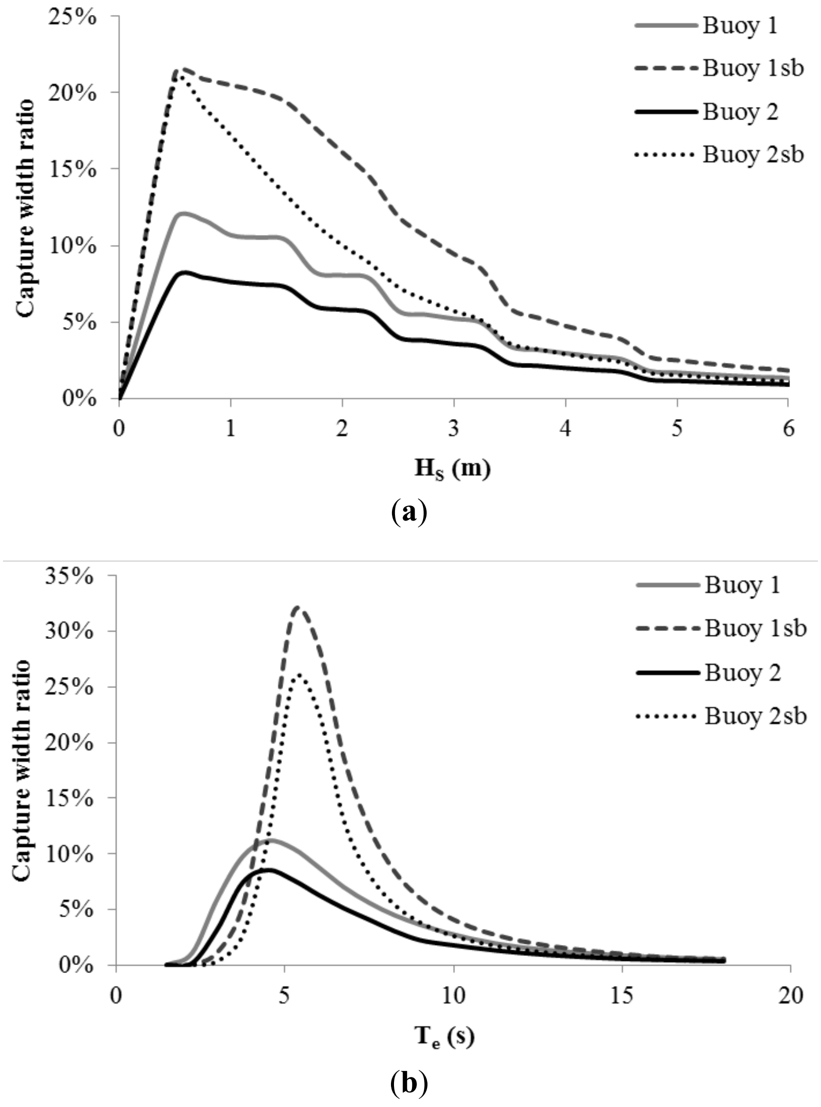

Figure 6. (**a**) Energy production; (**b**) degree of utilization; (**c**) capture width ratio of the buoy configurations at the study sites.

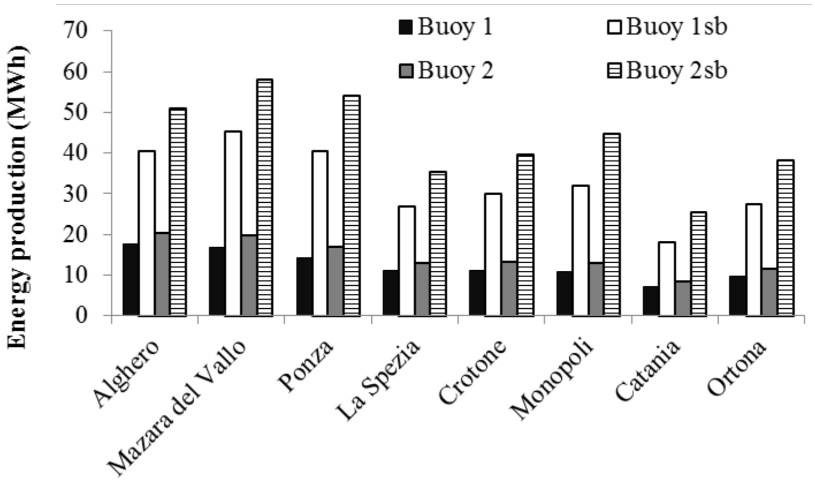

(**a**)

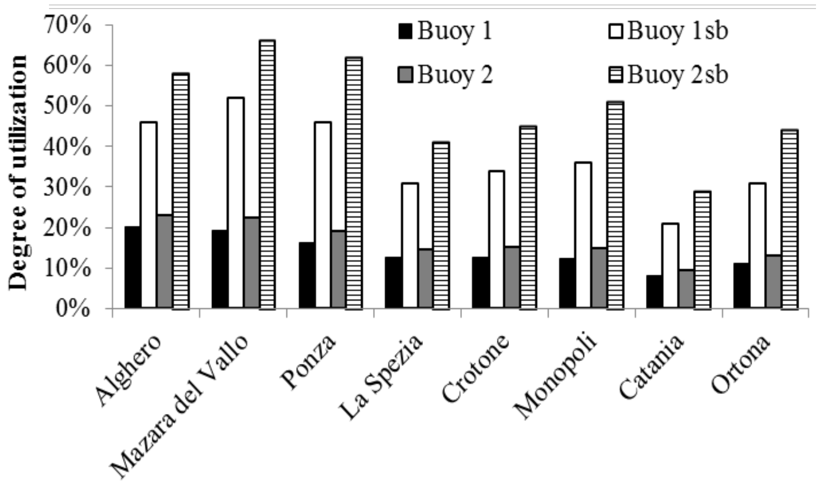

(**b**)

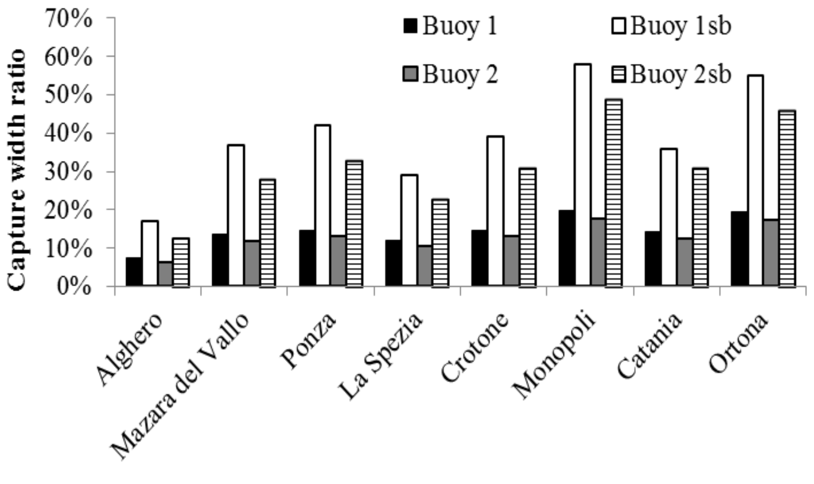

(**c**)

As expected, the largest buoy can extract more energy at each study location: the 5 m diameter buoy produces, on average, 20% more energy than the 3 m diameter one. The use of the submerged body allows the doubling of the energy production. Considering the largest buoy, the average annual energy production varies from 8 MWh at Catania to 20 MWh at Alghero for the single body system and from 25 MWh to 51 MWh for the two-body WEC. It is important to notice that the energy production is not monotonically increasing with the amount of available wave energy. For example, at Mazara del Vallo, the energy production is higher or equal to that at Alghero, despite that the site has a substantially less energetic wave climate (4.7 kW/m versus 9.1 kW/m). The same occurs for La Spezia and Monopoli, which greatly differ in wave energy availability, but have almost the same average annual energy production. Another example is represented by Ponza and La Spezia, which have the same average annual wave power (around 3.5 kW/m), but very different energy production (at Ponza, the device extracts 30% more energy). These results can easily be explained looking at the capture width data, which reveal that at some locations, the device is operating more optimally than in others. Considering the largest buoy, the capture width ratio of the single (dual) body system ranges from 6% (13%) at Alghero to 18% (49%) at Monopoli. Regarding the degrees of utilization, they are quite low for the conventional single body devices, except at the two most energetic sites (Alghero and Mazara del Vallo), where they are around 20%. However, they substantially increase when the floating body is connected to a submerged sphere, thanks to the resonant behavior of the WEC. The degree of utilization of the dual body devices is higher than 40% at most of the study sites, and it is maximum at Mazara del Vallo.

6. Discussion and Conclusions

Wave energy conversion has recently dominated the debate on renewable energies, due to its high potential, much higher than other green energy sources. Although its distribution throughout the planet is not homogeneous, even mild seas can be suitable for wave energy conversion, like in the Italian offshore. However, the mild wave climate of these locations requires a resizing of the conventional devices, which are usually designed to be deployed in the Atlantic, where wave potential is much higher. Such modifications tend to reduce the size of the single device and to deploy it in an array of several units, to take advantage of the less energetic wave climate without losing energy extraction capacity. A technology with these features is the Seabased WEC, a device designed by Uppsala University for deployment in the Swedish seas.

The aim of this work is to evaluate the Seabased device feasibility for wave energy exploitation under Mediterranean Sea conditions. A numerical model of the coupled buoy-generator system was developed to simulate the behavior of the wave energy converter in regular waves of different wave heights and periods. The simulated results, synthetized in terms of power matrices, are in good agreement with those obtained by Babarit *et al.* [44] for the same device. They presented very similar values of mean and maximum power output and a very much alike pattern, as well. Electricity production was estimated for two cylindrical buoys of different diameters at eight different locations off the Italian coasts. We also explored the effect of an additional submerged body connected to the floating buoy, which forces the system to be in resonance with the typical wave frequencies of the sites. The results were used to calculate the capture width ratio and the degree of utilization for each location, in order to assess the WEC performance and the economic feasibility of the hypothetical installations.

At Alghero and Mazara del Vallo, the degree of utilization of the conventional single body WEC range between 20% and 25%, showing that they can be suitable sites for wave energy exploitation. Moreover, adding a submerged object to the floating body would lead to a substantial increase of the degrees of utilization and would make this technology very attractive for wave energy exploitation in the Italian seas. In particular, the most favorable sites for this wave energy conversion technology seem to be Mazara del Vallo and Ponza.

Not much has been written about wave energy exploitation off the Italian coast; this analysis is meant to be a tool for future work aimed at choosing the right site and technology for wave energy conversion in the Italian seas. The model developed here is the starting point for future improvements, including (i) the time domain model with irregular wave inputs; (ii) mooring and foundations systems; (iii) power output smoothing; (iv) control strategies; and (v) parametric model optimization, depending on specific location, and last, but not least, the full costs analysis that determines the payback of the investment.

Acknowledgments

The authors would like to thank Giambattista Gruosso for his valuable advice on the electromagnetic modeling of the linear generator and the two anonymous reviewers for the useful comments and suggestions.

References

1. Leijon, M.; Bernhoff, H.; Berg, M.; Agren, O. Economical considerations of renewable electric energy production especially development of wave energy. *Renew. Energy* **2003**, *28*, 1201–1209.
2. Cruz, J. *Ocean Wave Energy*; Springer: Berlin, Germany, 2008.
3. Masuda, Y. Wave-Activated Generator. In Proceedings of the International Colloquium on the Exposition of the Oceans, Bordeaux, France, 3–5 March 1971.
4. McCormick, M.E. Analysis of a wave-energy conversion buoy. *J. Hydronaut.* **1974**, *8*, 77–82.
5. Budal, K.; Falnes, J. A resonant point absorber of ocean waves. *Nature* **1975**, *256*, 478–479.
6. Salter, S.H. Wave power. *Nature* **1974**, *249*, 720–724.
7. Falnes, J. A review of wave-energy extraction. *Mar. Struct.* **2007**, *20*, 185–201.
8. Clément, A.; McCullen, P.; Falcão, A.F.; Fiorentino, A.; Gardner, F.; Hammarlund, K.; Lemonis, G.; Lewis, T.; Nielsen, K.; Petroncini, S.; Pontes, M.T.; Schild, P.; Sjöström, B.O.; Sørnsen, H.C.; Thorpe, T. Wave energy in Europe: Current status and perspectives. *Renew. Sustain. Energy Rev.* **2002**, *6*, 405–431.
9. Arinaga, R.A.; Cheung, K.F. Atlas of global wave energy from 10 years of reanalysis and hindcast data. *Renew. Energy* **2012**, *39*, 49–64.
10. Gunn, K.; Stock-Williams, C. Quantifying the global wave power resource. *Renew. Energy* **2012**, *36*, 296–304.
11. Mollison, D.; Pontes, M.T. Assessing the Portuguese wave-power resource. *Energy* **1992**, *17*, 255–268.
12. Waters, R.; Engström, J.; Isberg, J.; Leijon, M. Wave climate off the Swedish west coast. *Renew. Energy* **2009**, *34*, 1600–1606.

13. Liberti, L.; Carillo, A.; Sannino, G. Wave energy resource assessment in the Mediterranean, the Italian perspective. *Renew. Energy* **2013**, *50*, 938–949.
14. Vicinanza, D.; Cappietti, L.; Ferrante, V.; Contestabile, P. Estimation of the wave energy in the Italian offshore. *J. Coast. Res.* **2011**, *64*, 613–617.
15. Falcão, A.F. Wave energy utilization: A review of the technologies. *Renew. Sustain. Energy Rev.* **2010**, *14*, 899–918.
16. Scruggs, J.; Jacob, P. Harvesting ocean wave energy. *Science* **2009**, *323*, 1176–1178.
17. Polinder, H.; Gardner, F.; Vriesema, B. Linear PM Generator for the Wave Energy Conversion in the AWS. In Proceedings of International Conference on Electrical Machines (ICEM), Espoo, Finland, 28–30 August 2000; p. 309.
18. Mueller, M.A. Electrical generators for direct drive wave energy converters. *IEE Proc. Gener. Transm. Distrib.* **2002**, *149*, 446–456.
19. Leijon, M.; Danielsson, O.; Eriksson, M.; Thorburn, K.; Bernhoff, H.; Isberg, J.; Sundeberg, J.; Ivanova, I.; Sjöstedt, E.; Ågren, O.; Karlsson, K.E.; Wolfbrandt, A. An electrical approach to wave energy conversion. *Renew. Energy* **2006**, *31*, 1309–1319.
20. AWS Ocean Energy. Available online: http:// www.awsocean.com (accessed on 11 January 2013).
21. Sea Based. Available online: http:// www.seabased.com (accessed on 11 January 2013).
22. Polinder, H.; Damen, M.E.C.; Gardner, F. Linear PM generator system for wave energy conversion in the AWS. *IEEE Trans. Energy Convers.* **2004**, *19*, 583–589.
23. Thorburn, K.; Bernhoff, H.; Leijon, M. Wave energy transmission system concepts for linear generator arrays. *Ocean Eng.* **2004**, *31*, 1339–1349.
24. Boccotti, P. Caisson for Absorbing Wave Energy. U.S. Patent PCT/IT99/00361, 17 September 2002.
25. TERNA. Available online: http://www.terna.it (accessed on 25 January 2013).
26. Archetti, R.; Bozzi, S.; Passoni, G. Feasibility Study of a Wave Energy Farm in the Western Mediterranean Sea: Comparison among Different Technologies. In Proceedings of the 30th International Conference on Ocean, Offshore and Arctic Engineering (OMAE), Rotterdam, The Netherlands, 19–24 June 2011; doi:10.1115/OMAE2011-49372.
27. Bozzi, S.; Archetti, R.; Passoni, G. Wave Energy Exploitation in Italian Seas: A Feasibility Study. In Proceedings of the 7th European Seminar OWEMES, Rome, Italy, 5–7 September 2012; pp. 187–195.
28. Bozzi, S.; Archetti, R.; Passoni, G. Wave electricity production in Italian offshore: A preliminary investigation. *Renew. Energy* **2013**, submitted for publication.
29. Thorburn, K.; Leijon, M. Farm size comparison with analytical model of linear generator wave energy converters. *Ocean Eng.* **2006**, *34*, 908–916.
30. Istituto Superiore per la Protezione e la Ricerca Ambientale [in Italian]. Available online: http://www.idromare.it (accessed on 23 January 2013).
31. Lockett, F.P. Mathematical Modelling of Wave Energy Systems. In Proceedings of 4th World Renewable Energy Congress (WREC), Denver, CO, USA, 15–21 June 1996.
32. McCabe, A.P.; Aggidis, G.A. Optimum mean power output of a point-absorber wave energy converter in irregular waves. *Proc. Inst. Mech. Eng. Part A* **2009**, *223*, 773–781.
33. Munson, B.R.; Young, D.F.; Okiishi, T.H. *Fundamentals of Fluid Mechanics*; John Wiley & Sons, Inc.: New York, NY, USA, 2009; pp. 519–535.

34. McCormick, M.E. *Ocean Engineering Mechanics with Applications*; Cambridge University Press: Cambridge, UK, 2009; pp. 273–375.
35. Waters, R.; Rahm, M.; Eriksson, M.; Svensson, O.; Srömstedt, E.; Boström, C.; Sundberg, J.; Leijon, M. Ocean wave energy absorption in response to wave period and amplitude—Offshore experiments on a wave energy converter. *IET Renew. Power Gener.* **2011**, *5*, 465–469.
36. Ferdinande, V.; Vantorre, M. Hydrodynamics of Ocean Wave-Energy Utilization. In *International Union of Theoretical and Applied Mechanics Symposium*; Springer: Berlin, Germany, 1985; pp. 217–226.
37. Alves, M.; Traylor, H.; Sarmento, A. Hydrodynamic Optimization of a Wave Energy Converter Using a Heave Motion Buoy. In Proceedings of the 7th European Wave and Tidal Energy Conference, Porto, Portugal, 11–14 September 2007.
38. Engström, J.; Eriksson, M.; Isberg, J.; Leijon, M. Wave energy converter with enhanced amplitude response at frequencies coinciding with Swedish west coast sea states by use of a supplementary submerged body. *J. Appl. Phys.* **2009**, *106*, 064512:1–064512:5.
39. Engström, J.; Kurupath, V.; Isberg, J.; Leijon, M. A resonant two body system for a point absorbing wave energy converter with direct-driven linear generator. *J. Appl. Phys.* **2011**, *110*, 124904:1–124904:8.
40. *ANSYS AQWA User Manual v.13.0*; Century Dynamics Ltd.: Horsham, UK, 2010.
41. Falnes, J. *Ocean Waves and Oscillating Systems*; Cambridge University Press: Cambridge, UK, 2002; pp. 1–275.
42. Eriksson, M.; Waters, R.; Svensson, O.; Isberg, J.; Leijon, M. Wave power absorption: Experiments in open sea and simulation. *J. Appl. Phys.* **2007**, *102*, 084910:1–084910:5.
43. Tyrberg, S.; Waters, R.; Leijon, M. Wave power absorption as a function of water level and wave height: theory and experiment. *IEEE J. Ocean. Eng.* **2010**, *35*, 558–564.
44. Babarit, A.; Hals, J.; Kurniawan, A.; Muliawan, M.; Moan, T.; Krokstad, J. Numerical estimation of wave energy delivery from a selection of wave energy converters. *Renew. Energy* **2012**, *241*, 44–63.
45. Hagerman, G.; Bedard, R. *Guidelines for Preliminary Estimation of Power Production by Offshore Wave Energy Conversion Devices*; Technical Report E2I EPRI-WP-US-001; Electricity Innovation Institute, Electric Power Research Institute: Palo Alto, CA, USA, 2003. http://resource.management6.com/E2I-EPRI-Specification-Guidelines-for-Preliminary-Estimation-of-download-w15280.pdf (last accessed on 22 January 2013).
46. Leijon, M.; Skoglund, A.; Waters, R.; Rehn, A.; Lindahl, M. On the physics of power, energy and economics of renewable electric energy sources—Part I. *Renew. Energy* **2010**, *35*, 1729–1734.
47. Skoglund, A.; Leijon, M.; Rehn, A.; Waters, R.; Lindahl, M. On the physics of power, energy and economics of renewable electric energy sources—Part II. *Renew. Energy* **2010**, *35*, 1735–1740.